Influence of the main operating parameters on the DRPSA process design based on the equilibrium theory

Ester Rossi, Giuseppe Storti & Renato Rota

Adsorption
Journal of the International Adsorption Society

ISSN 0929-5607
Volume 27
Number 1

Adsorption (2021) 27:27-39
DOI 10.1007/s10450-020-00274-9

Springer

Adsorption (2021) 27:27–39
https://doi.org/10.1007/s10450-020-00274-9

Influence of the main operating parameters on the DRPSA process design based on the equilibrium theory

Ester Rossi[1] · **Giuseppe Storti**[1] · **Renato Rota**[1]

Received: 6 July 2020 / Revised: 17 September 2020 / Accepted: 24 September 2020 / Published online: 12 October 2020

Abstract

Among the adsorption-based separation processes for gaseous mixtures, those exploiting pressure variations, so-called Pressure Swing Adsorption (PSA) processes, are the most popular. In this work, we focus on the specific PSA configuration known as Dual Reflux-Pressure Swing Adsorption (DR-PSA) given its ability to achieve sharp separations. In the case of binary mixtures, an analytical approach based on Equilibrium Theory has been proposed to identify the operating conditions for complete separation under the assumption of linear isotherms. This same approach is not available when the separation is not complete. Accordingly, in this work we study the features of non-complete separations by solving numerically a general DR-PSA model with parameter values suitable to approach equilibrium conditions (no mass transport resistances, no axial mixing, isothermal conditions and no pressure drop), thus reproducing the analytical solution when complete separations are examined. Even for non-complete separations, triangularly shaped regions at constant purity can be identified on a plane whose axes correspond to suitable design parameters. Moreover, we found a general indication on how to select the lateral feed injection position to limit the loss in product purities when complete separation is not established, whatever is the composition of the feeding mixture. Finally, a sensitivity analysis with respect to pressure ratio, light reflux ratio and heavy product flowrate is proposed in order to assess how to recover product purities according to the specific degrees of freedom of a DR-PSA apparatus.

Keywords Dual-reflux · PSA design · Gas separation · Cyclic adsorption process · Detailed numerical modelling · Non-complete separations

Abbreviations

A	Heavy component
B	Light component
BD	Blowdown step
C	Capacity ratio, $C = \frac{\beta_A t_{FE} \dot{n}_{LR} RT}{P_L V_{bed} \epsilon_T}$
D_{bed}	Diameter of the adsorption bed, m
d_p	Diameter of the solid particles, m
FE	Feed step
G	Reflux ratio, $G = \frac{\dot{n}_{LR}}{\dot{n}_{feed}}$
H_i	Linear isotherm constant for component i, $\frac{\text{mol}}{\text{kg Pa}}$
k_{LDF}	Linear driving force constant, s^{-1}
L_{bed}	Bed length, m
$n_{HP,T}$	Theorical heavy product number of moles produced in one cycle, mol
n_{LP}	Light product number of moles produced in one cycle, mol
n_{feed}	Number of moles fed in one cycle, mol
$\dot{n}$	Molar flowrate, $\frac{\text{mol}}{\text{s}}$
$\dot{n}_{feed}$	Lateral feed flowrate, $\frac{\text{mol}}{\text{s}}$
$\dot{n}_{HP}$	Heavy product flowrate, $\frac{\text{mol}}{\text{s}}$
$\dot{n}_{HP,T}$	Theorical heavy product flowrate, $\frac{\text{mol}}{\text{s}}$
$\dot{n}_{LP}$	Light product flowrate, $\frac{\text{mol}}{\text{s}}$
$\dot{n}_{LR}$	Light recycle flowrate, $\frac{\text{mol}}{\text{s}}$
N_c	Number of components
P	Pressure, Pa
PR	Pressurization step
PU	Purge step
q_i	Amount of i on the solid adsorbent, $\frac{\text{mol}}{\text{kg}}$
q_i^*	Amount of i on the solid adsorbent in equilibrium conditions, $\frac{\text{mol}}{\text{kg}}$

Electronic supplementary material The online version of this article (https://doi.org/10.1007/s10450-020-00274-9) contains supplementary material, which is available to authorized users.

✉ Renato Rota
renato.rota@polimi.it

[1] Chemistry, Materials and Chemical Engineering Department "Giulio Natta", Politecnico di Milano, Via Mancinelli 7, 20131 Milan, Italy

R Ideal gas constant, $\frac{\mathrm{j}}{\mathrm{molK}}$
S_Δ Triangular surface
T Temperature, K
t Time,s
t_0 Starting time of a step, s
u Superficial velocity, $u = \frac{volumetricflowrate}{area}, \frac{\mathrm{m}}{\mathrm{s}}$
u_{OUT} Superficial velocity in $Z = L$ during a given step
$y_{i,feed}$ Gas molar fraction of i in the lateral feed injection flow
$y_{i,H}$ Average gas molar fraction of i in ϑ_2
$y_{i,\mathrm{H}} = \frac{\int_{t_{0,\mathrm{BD}}}^{t_{0,\mathrm{BD}}+t_{BD}} \frac{u_{OUT\,BD} P_{BD} y_{BD,i}}{RT} dt + \int_{t_{0,PU}}^{t_{0,PU}+t_{PU}} \frac{u_{OUT\,PU} P_L y_{PU,i}}{RT} dt}{\int_{t_{0,\mathrm{BD}}}^{t_{0,BD}+t_{BD}} \frac{u_{OUT\,BD} P_{BD}}{RT} dt + \int_{t_{0,PU}}^{t_{0,PU}+t_{PU}} \frac{u_{OUT\,PU} P_L}{RT} dt}$
$y_{i,L}$ Average gas molar fraction of i in ϑ_1
$,y_{i,L} = \frac{\int_{t_{0,FE}}^{t_{0,FE}+t_{FE}} \frac{u_{OUT\,FE} P_H y_{i,OUT\,FE}}{RT} dt}{\int_{t_{0,FE}}^{t_{0,FE}+t_{FE}} \frac{u_{OUT\,FE} P_H}{RT} dt}$
$y_{i,OUTFE}$ Gas molar fraction of i in $Z = L$ during the FE step
y_i Gas molar fraction of i
z_{feed} Feed injection position, dimensionless $z_{feed} = Z_{feed}/z_{rif}$
z Axial coordinate, dimensionless $z = Z/z_{rif}$
Z_{feed} Axial coordinate of the lateral feed injection, m
Z Axial coordinate, m

Greek symbols

β Selectivty, $\beta_i = \frac{1}{1+\rho_S RTH_i\left(\frac{1-\varepsilon_T}{\varepsilon_T}\right)}$
ε_B Bed void fraction
ε_T Total void fraction, $\varepsilon_T = \varepsilon_B + \left(1-\varepsilon_P\right)\varepsilon_B$
ε_p Solid particles porosity
ρ_s Solid density, $\frac{\mathrm{kg}}{\mathrm{m}^3}$
ρ_B Bed density, $\rho_B = \left(1-\varepsilon_T\right)\rho_S, \frac{\mathrm{kg}}{\mathrm{m}^3}$
μ Dynamic viscosity, $Pa \cdot s$
π High pressure to low pressure ratio, $\frac{P_H}{P_L}$
ϑ_1 Tank 1
ϑ_2 Tank 2

Acronyms

PSA Pressure swing adsorption
DR-PSA Dual reflux-pressure swing adsorption
FVM Finite volume method
PDE Partial differential equation
ODE Ordinary differential equation
PR Pressurization step
FE Feed step
PU Purge step
BD Blowdown step
CSS Cyclic steady state

Subscripts

i Component i, $i = A$ or B
n n^{th} Computational node, $n = 1 \ldots N$
A Heavy component
B Light component
rif Reference value
$n \pm \frac{1}{2}$ Walls of the computational nodes n
BD Blowdown step
FE Feed step
PR Pressurization step
PU Purge step
H Highest value of the cycle
L Lowest value of the cycle
opt Optimal
R Ratio between actual parameter value and reference value
ET Equilibrium theory parameter value

1 Introduction

In recent years, economical and energy-efficient separation processes are more and more welcome since they represent a large part of the costs in chemical, petrochemical and related industry (Sholl and Lively 2016). In this frame, adsorption-based processes are an attractive option and the development of novel solid materials could further foster the profitability of this type of separations when compared to more traditional gas separation techniques (Agarwal et al. 2008). In the case of gaseous mixtures, great attention is currently paid to processes applying adsorbent regeneration by changing the operating pressure, so-called Pressure Swing Adsorption (PSA) processes. It has been demonstrated that the PSA technology can be successfully applied to several separations of industrial interest, such as hydrogen purification, air separation, CO_2 capture, and CH_4 upgrading (Grande 2012). Despite the large potential of PSA processes, a major thermodynamic limitation adversely affects the performances of their traditional configurations (Skarstrom 1959; Yoshida et al. 2003). Indeed, with reference to binary mixtures, usually only the pure light component (i.e., the least adsorbable, in the following referred to as B) or the heavy one (i.e., the most adsorbable, in the following referred to as A) can be produced.

To overcome this limitation, the alternative process version called Dual Reflux PSA (DR-PSA) has been proposed (Leavitt 1992). While relying on the basic features of PSA, complete separations are enabled by a lateral feed injection and two recycles (one of heavy and the other of light component). Following the first proposal, several papers explored different experimental applications of DR-PSA for separating different mixtures, namely: mixtures carrying CO_2 (Wawrzynczak et al. 2019; Shen 2017; Li et al. 2016; Kim et al. 2016; Sivakumar et al. 2011a, b; Takamura et al. 2001; Diagne et al. 1995, 1994;), N_2/O_2 (Wang et al. 2019; Tian et al. 2017), N_2/CH_4 (Weh et al. 2020; Xiao et al. 2019; Zhang et al. 2016; Salemann et al.

2015), and N_2/C_2H_6 (Mc Intyre 2002, 2010). This body of work built the basic understanding of the main features and capabilities of DR-PSA. The empirical tuning of some operating parameters has been proposed (May et al. 2017; Zhang et al. 2016; Saleman et al. 2015) to improve the separation performances, while innovative process configurations have been designed (cf. Tian et al. 2017; Sivakumar et al. 2011a, b) again with the final aim to maximize purity and recovery.

Similar efforts towards the design of the best process conditions have been made on the modelling side. Different models have been proposed, ranging from detailed models requiring numerical solutions (Rossi et al. 2019a, b; Zou et al. 2017; May et al. 2017; Bhatt et al. 2014; Thakur et al. 2011) to simplified semi-analytical models based on the so called *Equilibrium Theory* (Bhatt et al. 2018, 2017, 2013; Kearns and Webley, 2006a, b). In the latter case, the design conditions which allow the complete separation of binary mixtures in the case of linear isotherms have been investigated (Bhatt et al. 2013, 2015, 2017, 2018) and two key process parameters have been identified: the capacity ratio C, proportional to the ratio between the number of moles injected during the adsorption step and the volume of the column, and the dimensionless feed injection position z_{feed}. In the plane defined by these two parameters, a Triangular Operating Zone (TOZ) is established inside which complete separation is guaranteed (Bhatt et al. 2013). The TOZ is characterized by a single, constant value of a third parameter G (the reflux ratio, proportional to the ratio between the light reflux and the feed flowrate). Such an approach represents a first step towards the predictions of optimal separation conditions, but its validity is significantly limited by the assumptions of the Equilibrium Theory, with particular reference to the strong requirement of complete separation. However, in many practical processes complete separation is not required since purity values larger than a given target value usually suffice.

Therefore, the main aim of this work is to explore the role of the different process conditions on the separation performances retaining the main assumption behind the equilibrium model but *under conditions of non-complete separation*. In other words, based on the main results provided by the Equilibrium Theory (i.e., the identification of the TOZ), we analysed the process behaviour outside such a region through a detailed mathematical model. Extensive simulations with different operating conditions allowed identifying new triangular operating regions on the $C - z_{feed}$ plane at constant purity and non-complete separation. These results enable to understand the effects of different key process parameters (i.e., heavy product flowrate, light recycle ratio, and pressure ratio) in a quantitative way, thus providing effective guidelines to tune the separation performances also in the case of non-complete separations.

2 DR-PSA configuration

The DR-PSA process considered involves four steps performed by two identical beds working simultaneously. These steps are: (i) feed (FE), during which the gas mixture to be separated is fed to an adsorption bed at constant pressure; (ii) blowdown (BD), where the pressure is reduced from the highest value P_H to the lowest one P_L; (iii) purge (PU), in which the bed which was previously in FE is regenerated at constant pressure; and (iv) pressurization (PR), during which the pressure is raised again from P_L to P_H. Four different configurations of the process can be applied, based on the pressure of the FE step (P_H or P_L) and on the stream which is used for pressurization (A-rich or B-rich) (cf. Kearns and Webley 2006b). In this work, we focus on the configuration named DR-PH-A, where pressure switching is performed with the A-rich stream and the feed stream is injected at P_H. The corresponding half-cycle is sketched in Fig. 1, where the A-rich stream is indicated as "heavy product stream" and the B-rich stream as "light product stream". The lateral feed injection is represented in the figure by the molar flowrate $\dot{n}_{feed}$ and it is injected into the column at an intermediate position $z = z_{feed}$, where z is the dimensionless axial coordinate. As further detailed in (Rossi et al. 2019a), two tanks are involved in the specific process under examination, ϑ_1 and ϑ_2. The first tank, ϑ_1, is used to collect the B-rich stream leaving column 1 during FE and the two leaving streams are the light product and the light recycle to column 2 during PU, respectively. The second tank, ϑ_2, collects the A-rich stream during step PU of column 2 and step BD of column 1,

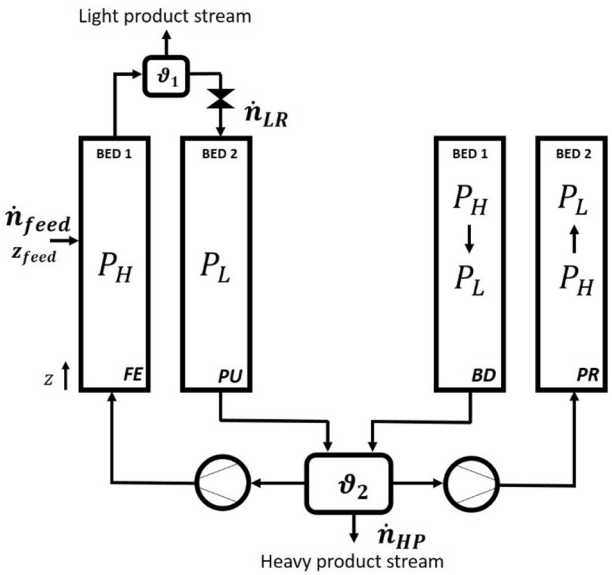

Fig. 1 Sketch of the first half-cycle of the process. During the second half, the two columns are exchanged

while the leaving streams are heavy product during PU and heavy recycle during BD, respectively. The molar fractions of the light product, $y_{i,L}$, and those of the heavy product, $y_{i,H}$, are computed as cycle average values of the molar fractions entering ϑ_1 and ϑ_2, respectively. The presence of the two tanks, with a large enough volume, is to tone down possible irregularities in the streams flowrates (Sivakumar and Rao 2011a; Rossi et al. 2019a).

3 Mathematical model, numerical approach and solving procedure

A detailed model has been developed and numerically solved as discussed elsewhere (Rossi et al. 2019a). A single-bed approach was applied, i.e., one single column is simulated all along the entire cycle (FE, BD, PU, and PR) while assuming that the two beds are identical. Notably, the simulation is carried out from an arbitrary initial condition until Cyclic Steady State (CSS) conditions are established, i.e., the model results of two subsequent cycles are identical in terms of integration variables according to a given tolerance.

The main model assumptions are:

- Ideal gas mixtures;
- Isothermal conditions;
- Mass transport between gas and solid phase described by the Linear Driving Force (LDF) model (Farooq et al. 1989);
- Pressure drops evaluated by the Blake-Kozeny equation (Thakur et al. 2011);
- Negligible axial dispersion, as expected in gas phase adsorption processes (Liao and Shiau 2000).

Model constitutive equations are summarized below for a binary mixture ($i = 1, 2$):

$$\varepsilon_T \frac{\partial P}{\partial t} + \frac{\partial (uP)}{\partial z} + \rho_B RT \sum_{i=1}^{2} \frac{\partial q_i}{\partial t} = 0 \tag{1}$$

$$\varepsilon_T \frac{\partial \left(P y_i\right)}{\partial t} + \frac{\partial \left(u P y_i\right)}{\partial z} + RT \rho_B \frac{\partial q_i}{\partial t} = 0 \tag{2}$$

$$\frac{\partial q_i}{\partial t} = k_{LDF,i}\left(q_i^* - q_i\right) \tag{3}$$

$$\frac{\partial P}{\partial z} = -\frac{u}{\frac{150}{4}\frac{1}{r_p^2}\left(\frac{1-\varepsilon_B}{\varepsilon_B}\right)^2 \mu} \tag{4}$$

They are total (1) and component (2) material balances, component material balances of the solid phase (3), and Blake-Kozeny Eq. (4). The evaluation of the solid phase concentration at equilibrium, q_i^*, is carried out through a suitable equilibrium isotherm. In this work, since we aim to extend the results of the Equilibrium Theory, linear adsorption isotherms (5) are considered:

$$q_i^* = H_i P y_i, \quad i = 1, 2 \tag{5}$$

The resulting system of Partial Differential Equations (PDEs) has been discretised in the spatial domain applying the Finite Volume Method (FVM) with first order upwind interpolations, Lagrange extrapolations, and Van Leer's Flux Limiters. This approach has been reported to efficiently reproduce the complex dynamics typical of transient adsorption processes (Casas et al. 2013; Haghpanah et al. 2013; LeVeque 2002; Webley and He 2000; Rossi et al. 2019a). Once discretised in space, the system of PDEs reduces to a set of Ordinary Differential Equations (ODEs) which has been integrated in time using Matlab® routine *ode15s*. A comprehensive summary of boundary and initial conditions is presented in Table S1 of the Supplementary Information. In particular, an air-like composition of the feed stream (i.e., $y_{A,feed} = 0.79$) has been considered.

All the reported simulations have been performed using a spatial grid made of 300 nodes. The grid independence of the results has been checked by comparison with the results corresponding to finer grid simulations (500 nodes). Moreover, the achievement of CSS conditions has been checked both in terms of accuracy of material balance closure and constant purity values of both the product streams.

4 Non-complete separation study

The separation of a binary mixture of oxygen and nitrogen using zeolite 5A as adsorbent is considered as case study. Realistic values of the process parameters have been selected, with the exception of those required to approach equilibrium conditions. Namely, very large values of transport coefficients and particle size have been applied in order to have negligible mass transport resistances and pressure drops, respectively.

In Table 1, the operating and process parameters for the case study with $y_{A,feed} = 0.79$ are reported.

Moreover, the definitions of the four main variables discussed in the following are summarized below:

$$G = \frac{\dot{n}_{LR}}{\dot{n}_{feed}} \quad \textit{Reflux ratio} \tag{6}$$

$$C = \frac{\beta_A t_{FE} \dot{n}_{LR} RT}{P_L V_{bed} \varepsilon_T} \quad \textit{Capacity ratio} \tag{7}$$

Table 1 Case-study parameter values

Parameter	Value	Units
P_H	2×10^5	Pa
P_L	1×10^5	Pa
$y_{A,feed}$	0.79	–
T	303.15	K
D	0.03	m
t_{FE}	400	s
ε_B	0.31	–
ε_P	0.65	–
ε_T	0.76	–
L	1	m
H_A	2.3×10^{-6}	mol/kg Pa
H_B	1×10^{-6}	mol/kg Pa
V_{bed}	7.07×10^{-4}	m^3
$\dot{n}_{feed}$	1.83×10^{-5}	mol/s
$\dot{n}_{HP}$	1.45×10^{-5}	mol/s
$\dot{n}_{LR}$	2.25×10^{-5}	mol/s

$$\pi = \frac{P_H}{P_L} \quad Pressure\ ratio \tag{8}$$

$$\beta_i = \frac{1}{1 + \rho_S RTH_i\left(\frac{1-\varepsilon_T}{\varepsilon_T}\right)} \quad Selectivity \tag{9}$$

Taking advantage of the semi-analytical solution based on Equilibrium Theory (Ebner and Ritter, 2004; Bhatt et al. 2013), the region of complete separation in the $C - z_{feed}$ plane (TOZ) is first evaluated, as shown in Fig. 2. At the chosen values of adsorption selectivity of each component (β_i), pressure ratio (π), and feed molar fraction ($y_{A,feed}$), any pair of values of the two operating parameters C and z_{feed} inside such a region results in complete separation (pure heavy and light components in each product stream). Note that this picture corresponds to a single value of the reflux ratio G, a quantity proportional to the ratio between the light reflux, $\dot{n}_{LR}$, and the feed flow rate, $\dot{n}_{feed}$.

The reliability of the detailed model for the conditions here investigated has been verified by simulating the process with the demanding (from a numerical point of view) operating conditions inside the TOZ indicated by the empty symbol in Fig. 2. The expected complete separation is correctly predicted by the detailed model, as clearly shown by the concentration profiles at CSS in Fig. 3. About 250 cycles are required to achieve CSS conditions from a column filled with the feeding mixture as initial condition. The material balances are also fulfilled with a residual error (relative to the fed mixture) for each component below 0.3%.

Let us now explore sets of operating conditions not corresponding to complete separation, that is, any pair of (C, z_{feed}) values outside the TOZ. In order to evaluate the sensitivity of the process performances to changes in the two key parameters (C, z_{feed}), all the conditions indicated by filled symbols in Fig. 2 have been simulated by keeping unchanged all the operating parameter values apart from C and z_{feed} (see Table 1; note that C values have been modified by changing only the duration of the feed step). Since FE time and distance from the column end become so small to be impractical for C values smaller than 0.0015 and for z_{feed} values smaller than 0.05, these regions were not investigated.

Note that the variation of C may be obtained also through the variation of other process parameters (cf. Eq. 7). However, once selected the solid adsorbent (and the

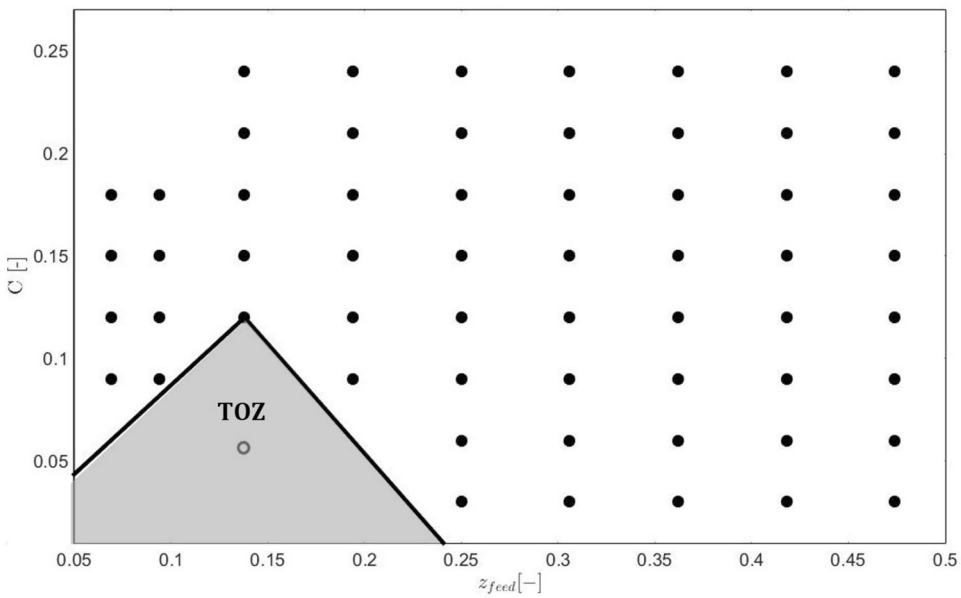

Fig. 2 TOZ and complete separation region. Symbols: the empty circle indicates the specific pair of $C - z_{feed}$ values considered in the preliminary model run; filled circles indicate the simulated operating conditions corresponding to incomplete separation

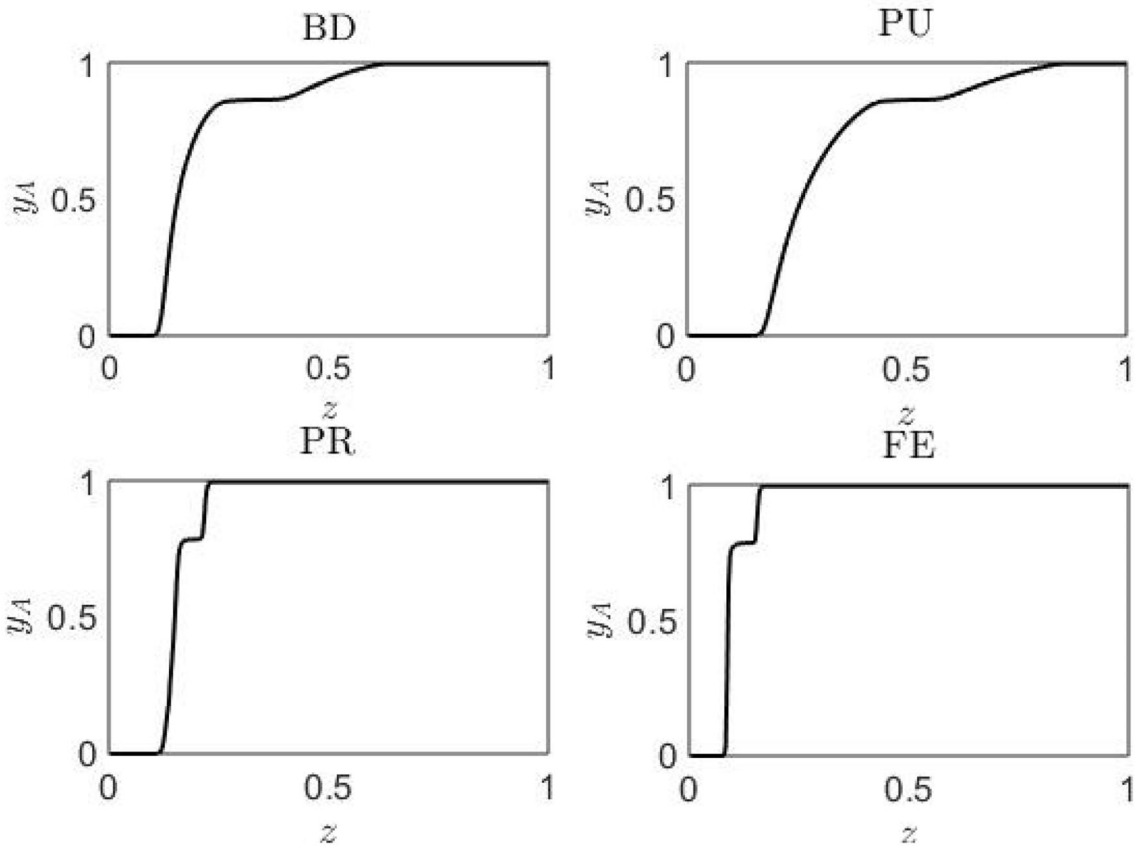

Fig. 3 Molar fraction profiles of component A as a function of z at the end of each step at CSS

corresponding properties), the value of the pressure ratio, and the unique G value estimated through the analytical solution based on Equilibrium Theory, we verified that the same results as those proposed in the following are obtained varying C through the variation of V_{bed}. Therefore, we consider these results meaningful whatever is the parameter used to change the C value, feed duration t_{FE} or bed volume V_{bed}.

The CSS purities of all the performed simulations are summarized in Table S2 of the Supplementary Information, while, in Table 2 the specific parameter values for the two other mixtures investigated are reported. Note that the parameters not reported in Table 2 have been set equal to those reported in Table 1.

Even though incomplete separation is predicted in all cases outside of the TOZ, the sensitivity of the purity of each component when changing C or z_{feed} is quite different. This is shown in Figs. 4 and 5 for light and heavy component where, taking advantage of the usual $C - z_{feed}$ representation, curves at constant purity are visualized. Note that, since discrete values are typically calculated, a proper interpolation of such data is required, as detailed in the Supplementary Information. Interestingly, these curves identify again

Table 2 Parameters for different feed mixtures

	$y_{A,feed} = 0.21$	$y_{A,feed} = 0.5$
C_{max}	0.14	0.13
G	2.04	1.56
z_{opt}	0.12	0.13
$\dot{n}_{feed}$	$1.30 \times 10^{-5} \frac{mol}{s}$	$1.56 \times 10^{-5} \frac{mol}{s}$
$\dot{n}_{HP}$	$0.27 \times 10^{-5} \frac{mol}{s}$	$0.78 \times 10^{-5} \frac{mol}{s}$
$\dot{n}_{LR}$	$2.65 \times 10^{-5} \frac{\text{mol}}{\text{s}}$	$2.43 \times 10^{-5} \frac{\text{mol}}{\text{s}}$

All the parameter values not reported are equal to that in Table 1

triangular regions inside which the product purity is larger than the purity specific of each curve. The vertex of the new triangles moves up and to the right at decreasing purity, i.e., higher productivity and z_{feed} values become feasible when the separation target is reduced. On the one hand, this behaviour results in a significant increase of the range of operating conditions which can be applied to achieve the selected separation performance. On the other hand, the variation of the purity of each component is much sharper at z_{feed} values smaller than that corresponding to the vertex than at larger values. Finally, the behaviour is quite asymmetric for the two

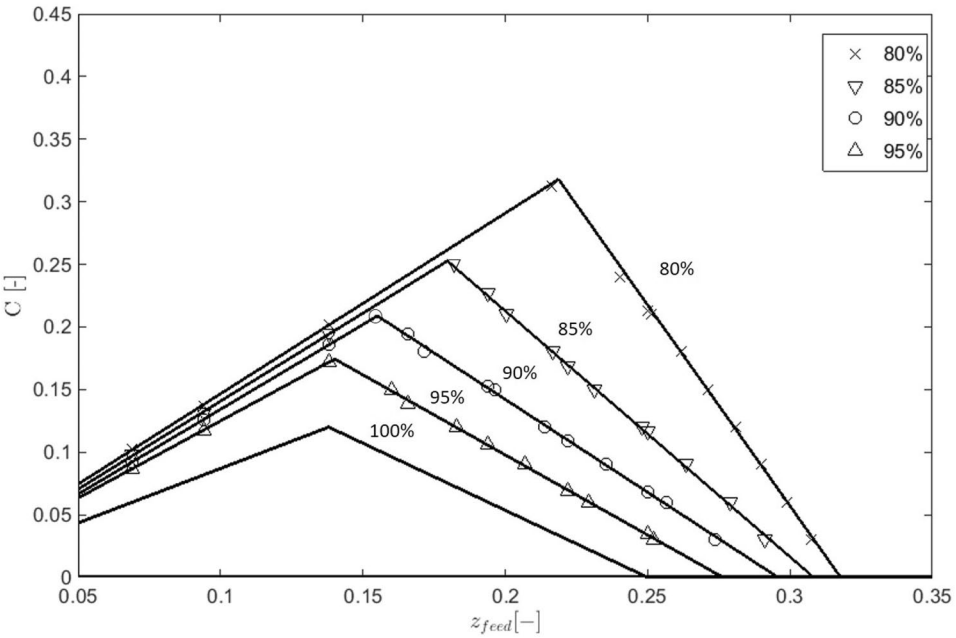

Fig. 4 Constant purity curves, light component ($y_{B,L}$). Symbols: predicted values; lines: data interpolation

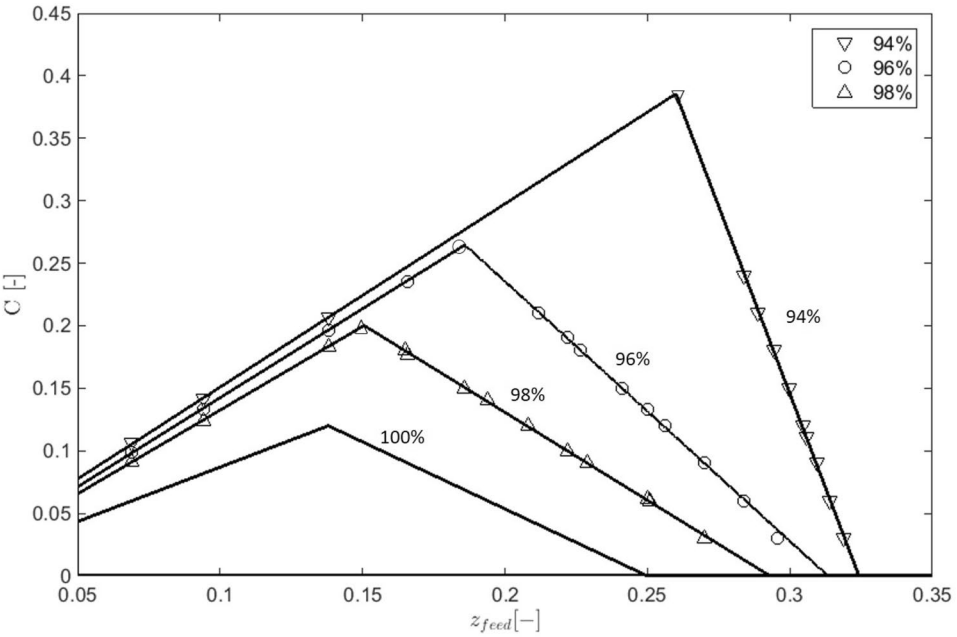

Fig. 5 Constant purity curves, heavy component ($y_{A,H}$). Symbols: predicted values; lines: data interpolation

components, being the sensitivity of the light component much larger than that of the heavy one.

This asymmetric behaviour can be easily explained through the overall material balances. Given the selected operating conditions (which involve product flowrates values of the light and heavy component suitable to achieve complete separation), the product flowrates are equal to $\dot{n}_{HP} = y_{A,feed} \cdot \dot{n}_{feed}$ and $\dot{n}_{LP} = y_{B,feed} \cdot \dot{n}_{feed} = (1 - y_{A,feed}) \cdot \dot{n}_{feed}$. Introducing these relations into the overall material balance of component *B* on a complete cycle, the following equation can be obtained:

$$\dot{n}_{feed} y_{B,feed} = \dot{n}_{feed} y_{A,feed} y_{B,H} + \dot{n}_{feed} \left(1 - y_{A,feed}\right) y_{B,L} \tag{10}$$

which, given the constraint $y_{B,feed} = 1 - y_{A,feed}$, can be readily rearranged as:

$$y_{B,L} = \frac{1 - 2y_{A,feed}}{1 - y_{A,feed}} + \frac{y_{A,feed}}{1 - y_{A,feed}} \cdot y_{A,H} \tag{11}$$

The last equation provides a linear relationship between the purity of the light component, $y_{B,L}$, and that of the heavy one, $y_{A,H}$, as a function of the specific feed composition.

Such relationship is shown in Fig. 6 for typical values of $y_{A,feed}$.

It is evident that the purities of light and heavy components are equal only when $y_{A,feed} = 0.5$, while they must be different for non-equimolar feed composition. More specifically, the variation of the light product purity must be larger than that of the heavy component when the feed mixture is richer in the heavy component, as in Figs. 4 and 5. Moreover, given the constraint represented by Eq. (11), the two figures are not independent. Accordingly, in the following we discuss the process performances with respect to the light component, with the exception of the cases in which $\dot{n}_{HP}$ is varied, that is, when Eq. (11) is not valid.

Figure 4 also shows a different sensitivity of the purity values depending on the feed positions being smaller or larger than that of the TOZ vertex. This behaviour has some practical implications. Even if the same purity can be achieved at feed positions larger and smaller than that of the TOZ vertex, larger feed positions should be highly preferred given their weaker sensitivity of the product purity to the variation of the process operating conditions (that is, in the position of the operating point in the $C - z_{feed}$ plane).

The same analysis has been repeated with different feed mixture composition. In particular, the two mixtures, $y_{A,feed} = 0.21$ and 0.50, have been investigated. TOZs have been identified (see Table 2 and Fig. S2 of the Supplementary Information) and several simulations have been performed to span the corresponding $C - z_{feed}$ plane. The obtained results fully confirm the general behaviour discussed above as well as the corresponding conclusions.

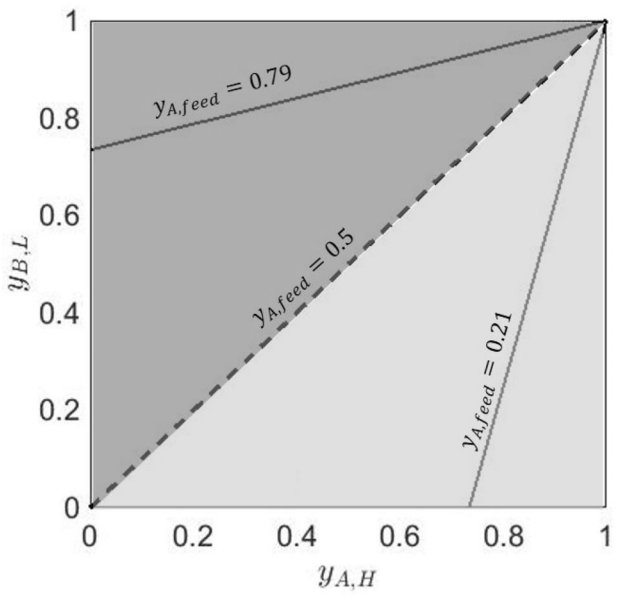

Fig. 6 Product purity values at different feed composition. The lighter grey surface refers to $y_{A,feed} < 0.5$, while the other to $y_{A,feed} > 0.5$

5 Process performance improvement

In the previous section, process conditions ensuring a given extent of separation have been identified starting from operating conditions provided by the simplified solution based on Equilibrium Theory (e.g., feed position, pressure ratio, recycle ratio, and adsorbent amount at given feed flowrate). In the following we discuss how to improve the separation performance of a given unit when keeping most of the design parameter values as predicted by the Equilibrium Theory but selecting operating conditions outside the TOZ. In the literature, the heavy product flowrate ($\dot{n}_{HP}$ in Fig. 1; Saleman et al. 2015; Zhang et al. 2016; May et al. 2017) and the light recycle ($\dot{n}_{LR}$ in Fig. 1; Bhatt et al. 2014; Shen et al. 2017; Zhang et al. 2016; Tian et al. 2017; Li et al. 2016) have been identified as major operating parameters to tune the product purity. On the other hand, the effect of changing the pressure ratio, π, has not been systematically investigated, even though it can be expected to affect significantly the DR-PSA process performances.

Three dimensionless variables, accounting for the change of the three process parameters mentioned above with respect to their values provided by the Equilibrium Theory, are defined as follows:

$$\alpha_R = \frac{\dot{n}_{HP}}{\dot{n}_{HP}^{ET}} \tag{12}$$

$$G_R = \frac{\dot{n}_{RL}}{\dot{n}_{RL}^{ET}} \tag{13}$$

$$\pi_R = \frac{\pi}{\pi^{ET}} \tag{14}$$

The first dimensionless parameter, α_R, involves the heavy product flowrate; the second one, G_R, the light reflux, and the last one, π_R, the pressure ratio. In all cases, the superscript ET indicates the reference value provided by the Equilibrium Theory for complete separation, i.e., the values considered in the previous sections (see Table 1 of the Supplementary Information). The impact of changing such values on the separation performances has been quantified considering three specific operating points in the usual $C - z_{feed}$ plane, as shown in Fig. 7.

The set of operating conditions labelled Run1 in Fig. 7 is located inside the TOZ, while that labelled Run2 corresponds to a lateral feed injected at z_{feed} larger than the optimal one, and Run3 corresponds to column shorter than the minimum value predicted by the Equilibrium Theory. While complete separation is achieved only in Run 1, the other two sets of conditions correspond to non-complete separation, as shown in Figs. 4 and 5. In the following, the impact of changes of the three dimensionless parameters

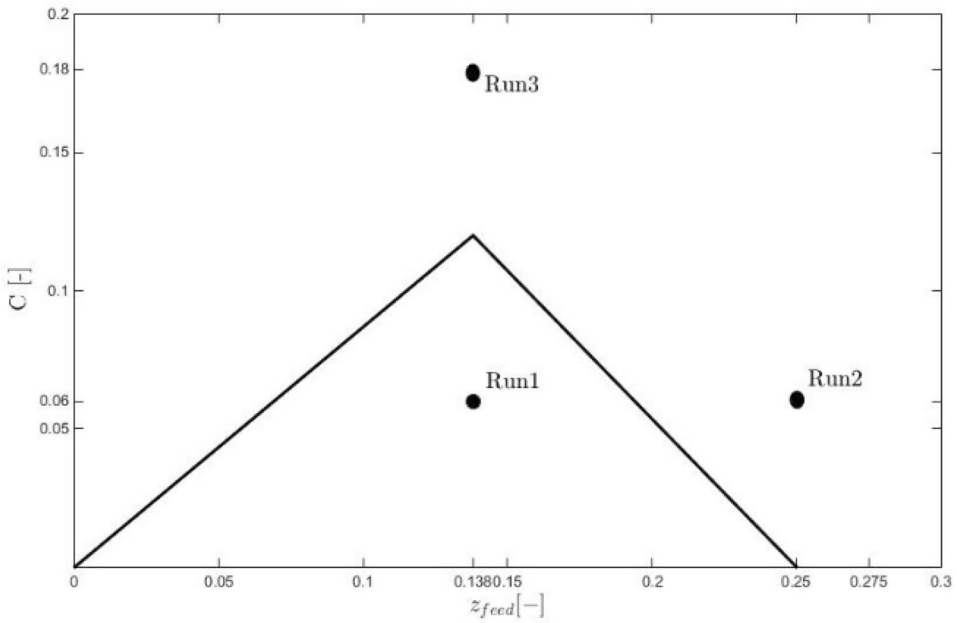

Fig. 7 Selected simulation conditions. Run1 (0.138, 0.06) inside, Run2 (0.275, 0.06) on the right side and Run3 (0.138, 0.18) above the TOZ

(Eqs. 12 to 14) will be explored: using Run 1 as reference, Runs 2 and 3 allow to check whether a partial separation recovery can be easily achieved outside the TOZ by changing only one of the parameters values provided by the Equilibrium Theory.

The results of this analysis are shown in Fig. 8, where the purities are reported as a function of the dimensionless operating parameters defined above.

For the cases of the variation of π and G (Fig. 8c and d) only the purity of B is reported. While, for the case of the variation of α_R, the purity of component A is reported too since, varying the heavy product molar flowrate, such a value cannot be computed through Eq. (11).

As expected, in the case of complete separation (Run1), the maximum purity value of $y_{B,L} = 1$ is invariably found at unitary value of the corresponding dimensionless parameter, i.e. when the operating conditions predicted by the equilibrium model are used. Hence, by increasing π, G, or α, an equal, or at least for values not too far from that provided by the Equilibrium Theory in the case of π, separation is obtained. This behaviour is imputable to the fact that Run1 lies in the TOZ region, which means complete separation when adopting π^{ET}, G^{ET} and $\dot{n}_{HP}^{ET}$.

For $\alpha_R < 1$, the molar flowrate extracted from tank ϑ_2 is inevitably lower than the amount of heavy component fed. Therefore, if a value smaller than $\dot{n}_{HP_T}$ is collected, the remaining portion of the heavy component fed becomes part of the light product stream, thus reducing the light product purity. Analogously, if $\alpha_R > 1$, $\dot{n}_{HP_T}$ is larger than the fed quantity of A and, therefore, part of the light component will be in the heavy product stream, reducing the heavy product purity. These behaviours are common to all the three runs considered, as shown by the three very similar results in Fig. 8a and b.

About the effect of π_R, a look at the concentration profiles inside the adsorption bed is helpful (cf. Fig. 9). In this work, the variation of π_R is obtained by changing the high pressure value of the cycle. Therefore, π_R smaller than 1 means lower P_H, that is smaller adsorbed amounts of both A and B, leading to poorer process performances as shown in Fig. 8c. On the other hand, the amount adsorbed rises for π_R values larger than 1. However, the shape of the concentration profiles in the adsorption beds changes too. As shown in Fig. 9a, the plateau at constant molar fraction shifts towards the end of the column and settles at larger mole fraction with respect to the case $\pi_R = 1$.

For values of the light recycle ratio lower than that provided by the Equilibrium Theory (*i.e.*, $G_R < 1$), the molar flowrate of the light component recycled in the purging column does not allow proper desorption. As a consequence, a larger amount of light component will be present in the heavy product stream extracted from the bed during the PU step. On the contrary, when raising G, better purge occurs, as shown by the profiles in Fig. 8d. However, at the same time, the increase of the purge molar flowrate pushes the concentration profiles more and more towards the end of the adsorption bed, leading to their eventual breakthrough.

6 Conclusions

Through an efficient numerical strategy together with a detailed mathematical model, the performances of the *Equilibrium Theory* – based design of a DR-PSA separation

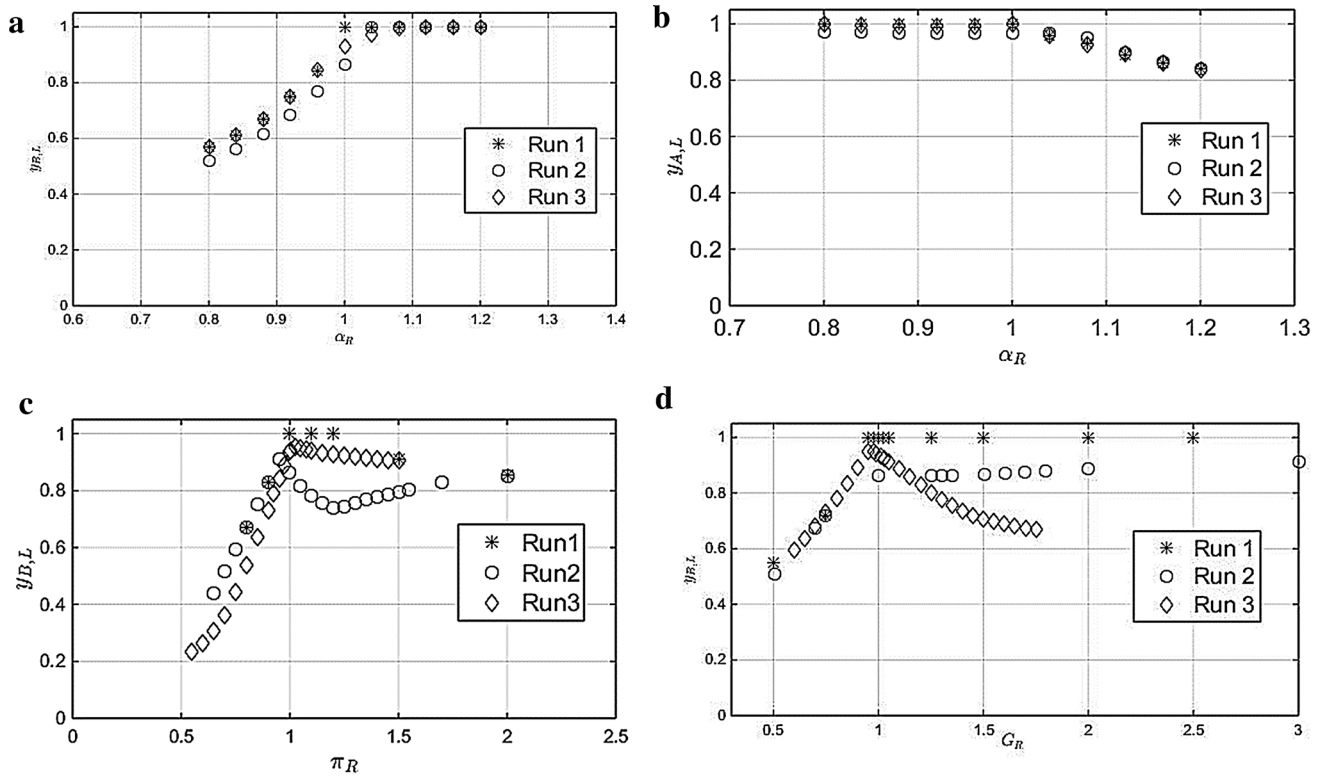

Fig. 8 Purity of component B in Run1, Run2, and Run3 as a function of α_R (**a**), π_R (**c**) and G_R (**d**). Purity of component A in Run1, Run2, and Run3 as a function of α_R (**b**)

process have been investigated. Even if all the results reported in this work have been obtained through a model implementing linear adsorption isotherms and using parameter values suitable to fulfil most of the assumptions behind the analytical solution based on *Equilibrium Theory*, some interesting general conclusions can be offered:

- for non-complete separations, regions leading to purity values larger than a given value have triangular shape in the operating plane $z_{feed} - C$, as those previously derived for complete separations, regardless the feed mixture composition;
- the loose of purity outside the TOZ is much sharper on the left of the optimal feed position (i.e., that of the vertex of the TOZ) than on the right; this means that for a practical process design, the feed position located on the right of the optimal value predicted by the Equilibrium Theory makes the process more robust;
- increasing the value of the heavy product flowrate allows for recovering (or at least for not losing, in case of operating conditions inside the TOZ) the light product purity; on the contrary, reducing the value of the heavy product flowrate enables the recovery (or at least not losing, in case of operating conditions inside the TOZ) the heavy product purity; this permits to tune the process performances to the desired target, also considering that the purity loss is larger for the component with lower feed concentration;
- changing the pressure ratio from the value provided by the Equilibrium Theory never results in improving the process performances; this means that increasing the pressure ratio for improving the separation requires retuning all the other process parameters according to Equilibrium Theory;
- similar conclusions arise for the light recycle ratio: changing its value from the one provided by the Equilibrium Theory does not allow for recovering better performance even in case of non-complete separation.

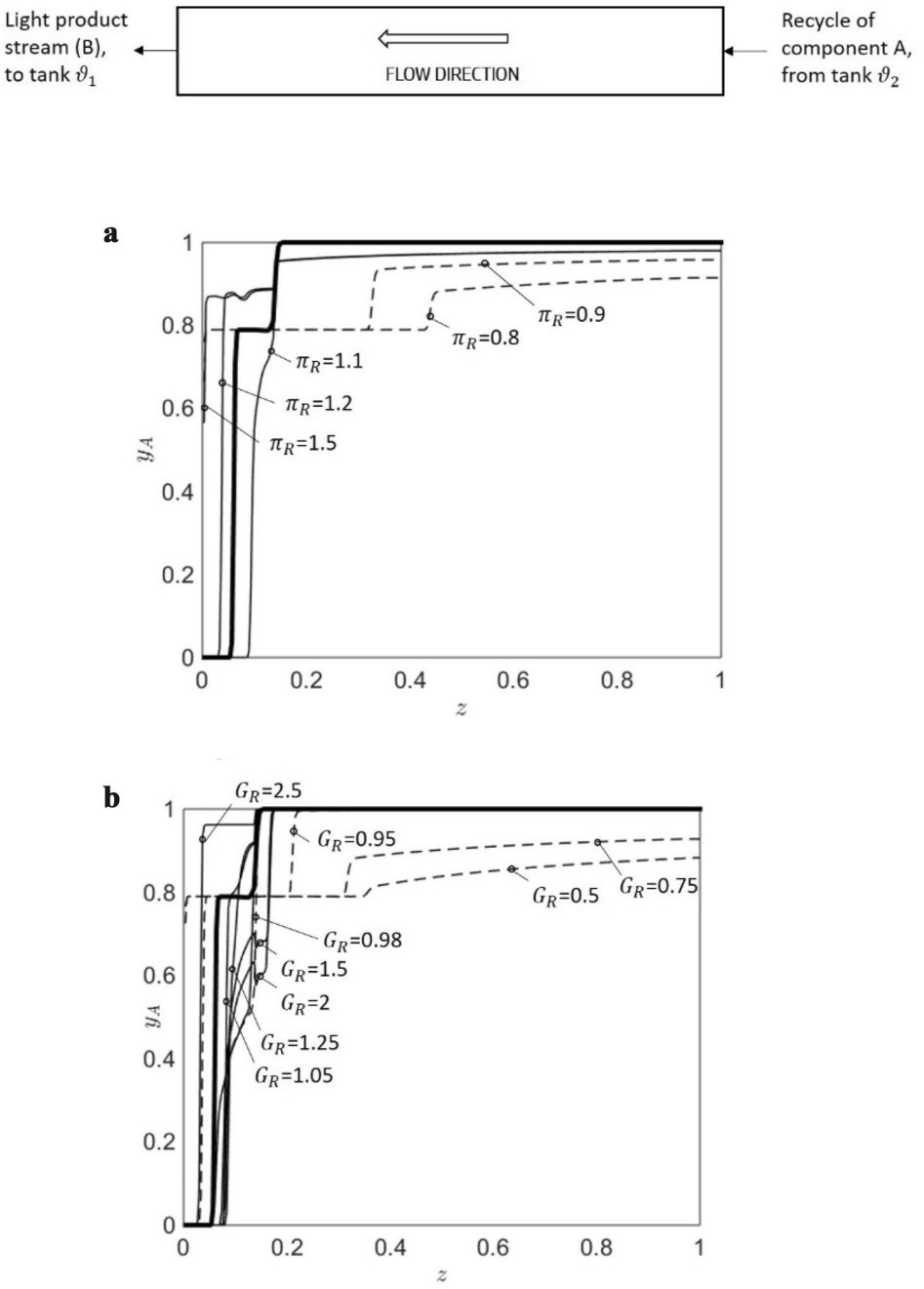

Fig. 9 Profiles of the heavy component gas mole fraction at the end of the feed step (Run1) when changing π_R (**a**) and G_R (**b**). (- -) parameter values smaller than the Equilibrium Theory value; (−) parameter values larger than the Equilibrium Theory value. Heavy lines refer to complete separation conditions (parameter value equal the Equilibrium Theory value)

Funding Open access funding provided by Politecnico di Milano within the CRUI-CARE Agreement.

References

Agarwal, A., Biegler, L.T., Zitney, S.E.: Simulation and optimization of pressure swing adsorption systems using reduced-order modeling. Ind. Eng. Chem. Res. **48**(5), 2327–2343 (2008)

Bhatt, T.S., Storti, G., Rota, R.: Optimal design of dual-reflux pressure swing adsorption units via equilibrium theory. Chem. Eng. Sci. **102**, 42–55 (2013)

Bhatt, T.S., Sliepcevich, A., Storti, G., Rota, R.: Experimental and modeling analysis of dual-reflux pressure swing adsorption process. Ind. Eng. Chem. Res. **53**(34), 13448–13458 (2014)

Bhatt, T.S., Storti, G., Rota, R.: Detailed simulation of dual-reflux pressure swing adsorption process. Chem. Eng. Sci. **122**, 34–52 (2015)

Bhatt, T.S., Storti, G., Denayer, J.F.M., Rota, R.: Optimal design of dual-reflux pressure swing adsorption units via equilibrium theory: process configurations employing heavy gas for pressure swing. Chem. Eng. J. **311**, 385–406 (2017)

Bhatt, T.S., Storti, G., Denayer, J.F., Rota, R.: Equilibrium theory-based assessment of dual-reflux pressure swing adsorption cycles that utilize light gas for pressure swing. Ind. Eng. Chem. Res. **58**(1), 350–365 (2018)

Casas, N., Schell, J., Joss, L., Mazzotti, M.: A parametric study of a PSA process for pre-combustion CO_2 capture. Sep. Purif. Technol. **104**, 183–192 (2013)

Diagne, D., Goto, M., Hirose, T.: New PSA process with intermediate feed inlet position operated with dual refluxes: Application to carbon dioxide removal and enrichment. J. Chem. Eng. Jpn. **27**(1), 85–89 (1994)

Diagne, D., Goto, M., Hirose, T.: Experimental study of simultaneous removal and concentration of CO_2 by an improved pressure swing adsorption process. Energy Convers. Manage. **36**(6–9), 431–434 (1995)

Ebner, A.D., Ritter, J.A.: Equilibrium theory analysis of dual reflux PSA for separation of a binary mixture. AIChE J. **50**(10), 2418–2429 (2004)

Farooq, S., Ruthven, D., Boniface, H.: Numerical simulation of a pressure swing adsorption oxygen unit. Chem. Eng. Sci. **44**(12), 2809–2816 (1989)

Grande, C.A.: Advances in pressure swing adsorption for gas separation. ISRN Chem. Eng. **2012**, 982934 (2012). https://doi.org/10.5402/2012/982934

Haghpanah, R., Majumder, A., Nilam, R., Rajendran, A., Farooq, S., Karimi, I.A., Amanullah, M.: Multiobjective optimization of a four-step adsorption process for postcombustion CO_2 capture via finite volume simulation. Ind. Eng. Chem. Res. **52**(11), 4249–4265 (2013)

Kearns, D.T., Webley, P.A.: Modelling and evaluation of dual reflux pressure swing adsorption cycles: Part II. Productivity and energy consumption. Chem. Eng. Sci. **61**(22), 7234–7239 (2006a)

Kearns, D.T., Webley, P.A.: Modelling and evaluation of dual-reflux pressure swing adsorption cycles: Part I. Mathematical models. Chem. Eng. Sci. **61**(22), 7223–7233 (2006b)

Kim, S., Ko, D., Moon, I.: Dynamic optimization of a dual pressure swing adsorption process for natural gas purification and carbone capture. Ind. Eng. Chem. Res. **48**, 12444–12451 (2016)

Leavitt, F. W.: Duplex adsorption process. US Patent 5,085,674 1992.

Leveque, R.J.: *Finite Volume Methods for Hyperbolic Problems*. Cambridge: Cambridge University Press (2002)

Li, D., Zhou, Y., Shen, Y., Sun, W., Fu, Q., Yan, H., Zhang, D.: Experiment and simulation for separating CO_2/N_2 by dual-reflux pressure swing adsorption process. Chem. Eng. J. **297**, 315–324 (2016)

Liao, H., Shiau, C.: Analytical solution to an axial dispersion model for the fixed-bed adsorber. AIChE J. **46**(6), 1168–1176 (2000)

May, E.F., Zhang, Y., Saleman, T.L.H., Xiao, G., Li, G.K., Young, B.R.: Demonstration and optimisation of the four dual-reflux pressure swing adsorption configurations. Sep. Purif. Technol. **177**, 161–175 (2017)

Mc Intyre, J.A., Holland, C.E., Ritter, J.A.: High enrichment and recovery of dilute hydrocarbons by dual-reflux pressure-swing adsorption. Ind. Eng. Chem. Res. **41**(14), 3499–3504 (2002)

Mcintyre, J.A., Ebner, A.D., Ritter, J.A.: Experimental study of a dual reflux enriching pressure swing adsorption process for concentrating dilute feed streams. Ind. Eng. Chem. Res. **49**(4), 1848–1858 (2010)

Rossi, E., Paloni, M., Storti, G., Rota, R.: Modeling dual refluxpressure swing adsorption processes: numerical solution based on the finite volume method. Chem. Eng. Sci. **203**, 173–185 (2019a)

Rossi, E., Storti, G., Rota, R.: Optimal design procedure of dual-reflux pressure swing adsorption units for nonlinear separations. Ind. Eng. Chem. Res. **58**(16), 6644–6652 (2019b)

Saleman, T.L., Li, G.K., Rufford, T.E., Stanwix, P.L., Chan, K.I., Huang, S.H., May, E.F.: Capture of low grade methane from nitrogen gas using dual-reflux pressure swing adsorption. Chem. Eng. J. **281**, 739–748 (2015)

Shen, Y., Zhou, Y., Li, D., Fu, Q., Zhang, D., Na, P.: Dual-reflux pressure swing adsorption process for carbon dioxide capture from dry flue gas. Int. J. Greenhouse Gas Control **65**, 55–64 (2017)

Sholl, D.S., Lively, R.P.: Seven chemical separations to change the world. Nature **532**(7600), 435–437 (2016)

Sivakumar, S.V., Rao, D.P.: Modified duplex PSA. 1. Sharp separation and process intensification for CO2-N2–13X zeolite system. Ind. Eng. Chem. Res. **50**(6), 3426–3436 (2011a)

Sivakumar, S.V., Rao, D.P.: Modified duplex PSA 2 sharp separation and process intensification for N2–O2–5A zeolite system. Ind. Eng. Chem. Res. **50**(6), 3437–3445 (2011b)

Skarstrom, C.W.: Use of adsorption phenomena in automatic plant-type gas analyzers. Ann. N. Y. Acad. Sci. **72**(13), 751–763 (1959)

Takamura, Y., Narita, S., Aoki, J., Hironaka, S., Uchida, S.: Evaluation of dual-bed pressure swing adsorption for CO_2 recovery from boiler exhaust gas. Sep. Purif. Technol. **24**(3), 519–528 (2001)

Thakur, R.S., Kaistha, N., Rao, D.P.: Process intensification in duplex pressure swing adsorption. Comput. Chem. Eng. **35**(5), 973–983 (2011)

Tian, C., Fu, Q., Ding, Z., Han, Z., Zhang, D.: Experiment and simulation study of a dual-reflux pressure swing adsorption process for separating N_2/O_2. Sep. Purif. Technol. **189**, 54–65 (2017)

Wang, Y., An, Y., Ding, Z., Shen, Y., Tang, Z., Zhang, D.: Integrated VPSA processes for air separation based on dual reflux configuration. Ind. Eng. Chem. Res. **58**, 6562−6575 (2019)

Wawrzyńczak, D., Majchrzak-Kucęba, I., Srokosz, K., Kozak, M., Nowak, W., Zdeb, J., Smółka, W., Zajchowski, A.: The pilot dual-reflux vacuum pressure swing adsorption unit for CO_2 capture from flue gas. Sep. Purif. Technol. **209**, 560–570 (2019)

Webley, P.A., He, J.: Fast solution-adaptive finite volume method for PSA/VSA cycle simulation; 1 single step simulation. Comput. Chem. Eng. **23**(11–12), 1701–1712 (2000)

Weh, R., Xiao, G., Islam, M.A., May, E.F.: Nitrogen rejection from natural gas by dual reflux-pressure swing adsorption using activated carbon and ionic liquidic zeolite. Sep. Purif. Technol. **235**, 116215 (2020)

Xiao, G., Saleman, T.L., Zou, Y., Li, G., May, E.F.: Nitrogen rejection from methane using dual-reflux pressure swing adsorption with a kinetically-selective adsorbent. Chem. Eng. J. **372**, 1038–1046 (2019)

Yoshida, M., Ritter, J.A., Kodama, A., Goto, M., Hirose, T.: Enriching reflux and parallel equalization PSA process for concentrating trace components in air. Ind Eng Chem Res **8**, 1795–1803 (2003)

Zhang, Y., Saleman, T.L.H., Li, G.K., Xiao, G., Young, B.R., May, E.F.: Non-isothermal numerical simulations of dual reflux

pressure swing adsorption cycles for separating $N_2 + CH_4$. Chem. Eng. J. **292**, 366–381 (2016)
Zou, Y., Xiao, G., Li, G., Lu, W., May, E.F.: Advanced non-isothermal dynamic simulations of dual reflux pressure swing adsorption cycles. Chem. Eng. Res. Des. **126**, 76–88 (2017)